

Evidence for Luminosity Evolution of Long Gamma-ray Bursts in *Swift* Data

R. Salvaterra¹, C. Guidorzi¹, S. Campana¹, G. Chincarini^{1,2}, G. Tagliaferri¹

¹ *INAF, Osservatorio Astronomico di Brera, via E. Bianchi 46, I-23807 Merate (LC), Italy*

² *Dipartimento di Fisica G. Occhialini, Università degli Studi di Milano Bicocca, Piazza della Scienza 3, I-20126 Milano, Italy*

28 October 2018

ABSTRACT

We compute the luminosity function (LF) and the formation rate of long gamma ray bursts (GRBs) by fitting the observed differential peak flux distribution obtained by the BATSE experiment in two different scenarios: i) the GRB luminosity evolves with redshift and ii) GRBs form preferentially in low-metallicity environments. In both cases, model predictions are consistent with the *Swift* number counts and with the number of detections at $z > 2.5$ and $z > 3.5$. To discriminate between the two evolutionary scenarios, we compare the model results with the number of luminous bursts (i.e. with isotropic peak luminosity in excess of 10^{53} erg s⁻¹) detected by *Swift* in its first three years of mission. Our sample conservatively contains only bursts with good redshift determination and measured peak energy. We find that pure luminosity evolution models can account for the number of sure identifications. In the case of a pure density evolution scenario, models with $Z_{th} > 0.3 Z_{\odot}$ are ruled out with high confidence. For lower metallicity thresholds, the model results are still statistically consistent with available lower limits. However, many factors can increase the discrepancy between model results and data, indicating that some luminosity evolution in the GRB LF may be needed also for such low values of Z_{th} . Finally, using these new constraints, we derive robust upper limits on the bright-end of the GRB LF, showing that this cannot be steeper than ~ 2.6 .

Key words: gamma-ray: burst – stars: formation – cosmology: observations.

1 INTRODUCTION

Gamma Ray Bursts (GRBs) are powerful flashes of high-energy photons occurring at an average rate of a few per day throughout the universe. Their luminosity is such that they can be detected up to very high redshift (the current record is GRB 080913 at $z = 6.7$; Greiner et al. 2008). The energy source of a GRB is believed to be associated to the collapse of the core of a massive star in the case of long-duration GRBs, and due to merger- or accretion-induced collapse for the short-hard class of GRBs (see Mészáros 2006 for a recent review). In this paper, we limit our analysis to the class of long-duration GRBs.

The knowledge of GRBs has enormously benefited from the observations of the *Swift* satellite (Gehrels et al. 2004). Although the current sample of GRBs with known redshift is still too poor to allow a direct measure of the GRB luminosity function (LF), important constraints on the cosmic evolution of these sources can be set on the basis of recent *Swift* results. In particular, Salvaterra & Chincarini (2007, hereafter SC07) showed that models in which GRBs are unbiased tracer of cosmic star formation and are

characterised by a constant LF are robustly ruled out by the number of GRB detections at $z > 2.5$ and $z > 3.5$. Similar conclusions were reached recently by other studies (e.g. Guetta, Piran & Waxman 2005; Daigne et al. 2006; Cen & Fang 2007; Kistler et al. 2008). Moreover, they have shown that *Swift* data can be reproduced assuming luminosity evolution of the GRB LF (see also Lloyd-Ronning, Fryer & Ramires-Ruiz 2002; Wei & Gao 2003; Daigne et al. 2006) and/or that GRBs form preferentially in low metallicity environments (see also Natarajan et al. 2005; Langer & Norman 2006; Li 2007; Cen & Fang 2007; Lapi et al. 2008).

In this Letter, we derive the formation efficiency and the free parameters describing the GRB LF by fitting the differential peak flux distribution of BATSE GRBs in these two scenarios. We then obtain new and tighter constraints on the cosmic evolution of long GRBs by comparing different models against the number of luminous (i.e. with isotropic peak luminosities $L \gtrsim 10^{53}$ erg s⁻¹) GRBs detected by *Swift*. We also consider models with joint luminosity and density evolution providing a robust upper limit on the steepness of the bright-end of the GRB LF.

This Letter is organised as follows. In Section 2, we

briefly describe the different models and the main equations used in the calculation of the LF, and in Section 3, we compare model results against *Swift* data. Finally, we summarise our findings in Section 4.

2 MODEL DESCRIPTION

The observed photon flux, P , in the energy band $E_{\min} < E < E_{\max}$, emitted by an isotropically radiating source at redshift z is

$$P = \frac{(1+z) \int_{(1+z)E_{\min}}^{(1+z)E_{\max}} S(E) dE}{4\pi d_L^2(z)}, \quad (1)$$

where $S(E)$ is the differential rest-frame photon luminosity of the source, and $d_L(z)$ is the luminosity distance. To describe the typical burst spectrum we adopt the functional form proposed by Band et al. (1993), i.e. a smoothly broken power-law with a low-energy spectral index α , a high-energy spectral index β , and a break energy $E_b = (\alpha - \beta)E_p/(2 + \alpha)$, with $\alpha = -1$ and $\beta = -2.25$ (Preece et al. 2000, Kaneko et al. 2006). The spectrum normalisation is obtained by imposing that the isotropic-equivalent peak luminosity is $L = \int_{1 \text{ keV}}^{10000 \text{ keV}} ES(E)dE$. In order to broadly estimate the peak energy of the spectrum, E_p , for a given L , we assumed the validity of the correlation between E_p and L (Yonetoku et al. 2004, Ghirlanda et al. 2005), which is basically a different expression of the $E_p - E_{\text{iso}}$ relation (Amati et al. 2002, Amati 2006).

$$E_p = 337 \text{ keV} \left(\frac{L}{2 \times 10^{52} \text{ erg s}^{-1}} \right)^{0.49}. \quad (2)$$

Although the above correlation has an appreciable scatter, we will show that this does not affect our results.

Given a normalised GRB LF, $\phi(L)$, the observed rate of bursts with peak flux between P_1 and P_2 is

$$\begin{aligned} \frac{dN}{dt}(P_1 < P < P_2) &= \int_0^\infty dz \frac{dV(z)}{dz} \frac{\Delta\Omega_s}{4\pi} \frac{\Psi_{\text{GRB}}(z)}{1+z} \\ &\times \int_{L(P_1, z)}^{L(P_2, z)} dL' \phi(L'), \end{aligned} \quad (3)$$

where $dV(z)/dz = 4\pi cd_L^2(z)/[H(z)(1+z)^2]$ is the comoving volume element^{*}, and $H(z) = H_0[\Omega_M(1+z)^3 + \Omega_\Lambda + (1 - \Omega_M - \Omega_\Lambda)(1+z)^2]^{1/2}$. $\Delta\Omega_s$ is the solid angle covered on the sky by the survey, and the factor $(1+z)^{-1}$ accounts for cosmological time dilation. Finally, $\Psi_{\text{GRB}}(z)$ is the comoving burst formation rate. In this work, we model the GRB LF with a power law with an exponential cut-off at low luminosities:

$$\phi(L) \propto \left(\frac{L}{L_{\text{cut}}} \right)^{-\xi} \exp\left(-\frac{L}{L}\right). \quad (4)$$

SC07 have shown that models in which GRB form proportionately to the star formation rate (SFR) and are described by a LF constant in redshift are robustly ruled out by the number of GRB with sure detection at $z > 2.5$ and

^{*} We adopted the 'concordance' model values for the cosmological parameters: $h = 0.7$, $\Omega_m = 0.3$, and $\Omega_\Lambda = 0.7$.

Pure Luminosity Evolution Models				
δ	$k_{\text{GRB}}/(10^{-8} \text{M}_\odot^{-1})$	$L_0/(10^{51} \text{ erg s}^{-1})$	ξ	χ_r^2
1.5	1.07±0.11	0.66±0.21	2.16±0.09	0.95
2.0	1.01±0.10	0.36±0.08	2.08±0.06	0.83
2.5	0.94±0.09	0.20±0.04	2.03±0.05	0.92
3.0	0.94±0.09	0.10±0.02	1.99±0.04	0.84
Pure Density Evolution Models				
Z_{th}/Z_\odot	$k_{\text{GRB}}/(10^{-8} \text{M}_\odot^{-1})$	$L_0/(10^{51} \text{ erg s}^{-1})$	ξ	χ_r^2
0.1	11.38±1.60	10.34±4.10	2.51±0.22	0.81
0.2	4.45±0.68	8.40±3.58	2.48±0.22	0.78
0.3	2.80±0.45	7.40±3.11	2.50±0.22	0.80

Table 1. Best-fit parameters for different models: top panel for pure luminosity evolution and bottom panel for pure density evolution. Errors are at 1σ level.

$z > 3.5$ during the first two years of *Swift* mission. Thus, GRBs should have experienced some kind of evolution, being more luminous or more common in the past. Therefore we consider here two families of models: (i) luminosity evolution models, where the cut-off luminosity in the GRB LF varies as $L_{\text{cut}} = L_0(1+z)^\delta$ and (ii) density evolution models, where GRBs form preferentially in galaxies with metallicity below a given threshold Z_{th} . In the first case, the GRB formation rate is simply proportional to the global SFR, i.e. $\Psi_{\text{GRB}}(z) = k_{\text{GRB}}\Psi_*(z)$. We use here the recent determination of the SFR obtained by Hopkins & Beacom (2006), slightly modified to match the observed decline of the SFR with $(1+z)^{-3.3}$ at $z \gtrsim 5$ suggested by recent deep-field data (Stark et al. 2006). For the density evolution models, the GRB formation rate is obtained by convolving the observed SFR with the fraction of galaxies at redshift z with metallicity below Z_{th} using the expression computed by Langer & Norman (2006). In this scenario, the cut-off luminosity is assumed to be constant in redshift, i.e. $L_{\text{cut}} = \text{const} = L_0$.

Furthermore, we consider a third family of models in which both effects are presented: GRBs form preferentially in environments with $Z \leq Z_{th}$ and are characterised by an evolving LF.

3 LUMINOSITY vs DENSITY EVOLUTION

The free parameters in our model are the GRB formation efficiency k_{GRB} , the cut-off luminosity at $z = 0$, L_0 , and the LF power index ξ . We optimised the value of these parameters by χ^2 minimisation over the observed differential number counts in the 50–300 keV band of BATSE. We use here the results by Stern et al. (2000), who considered both triggered and non-triggered bursts and also corrected the distribution taking into account the BATSE detector efficiency. The best-fit parameters are reported in Table 1. As already pointed out by SC07, it is always possible to find a good agreement between models and data. Moreover, it is possible to reproduce also the differential peak flux count distribution in the 15–150 keV *Swift* band using the same GRB LF and formation efficiency obtained by fitting the

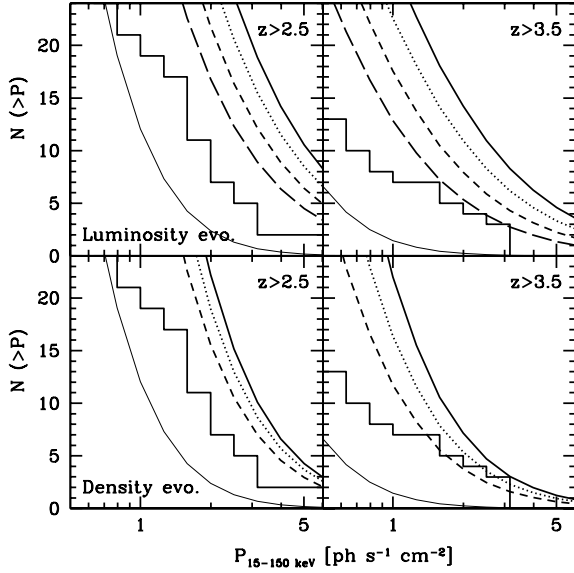


Figure 1. Cumulative number of GRBs at $z > 2.5$ (left panels) and $z > 3.5$ (right panels) as a function of the photon flux P . The no-evolution case is shown with the solid thin line. Top panels refer to luminosity evolution models: solid line is for $\delta = 3$, dotted line for $\delta = 2.5$, short-dashed line for $\delta = 2$, and long-dashed line for $\delta = 1.5$. Bottom panels refer to density evolution models: solid line is for $Z_{th} = 0.1 Z_{\odot}$, dotted line is for $Z_{th} = 0.2 Z_{\odot}$, and short-dashed line is for $Z_{th} = 0.3 Z_{\odot}$. The number of bursts detected by *Swift* in three years is shown as solid histogram. Note that the observed detections are lower limits, since many high- z GRBs can be missed by optical follow-up searches. A field of view of 1.4 sr for *Swift*/BAT is adopted.

BATSE data. Consistently with SC07, we find that the number of GRBs confirmed at $z > 2.5$ and $z > 3.5$ in the three years of *Swift* mission requires some kind of evolution. The results are shown in Fig. 1 for different evolution models. As a comparison, we show also the result for the no-evolution model with the solid thin line. The chance probability associated to the no-evolution model is found to be less than 10^{-4} ensuring that this kind of model can be discarded at a very high confidence level and indicating the need of some kind of evolution to explain *Swift* high- z detections (see also SC07).

In this work we highlight a new toll to discriminate between these two evolution scenarios by computing the number of luminous GRBs, i.e. bursts with isotropic peak luminosity $L \geq 10^{53}$ erg s^{-1} in the 1-10000 keV band. The model predictions are obtained by

$$\frac{dN}{dt}(> L) = \int_0^{\infty} dz \frac{dV(z)}{dz} \frac{\Delta\Omega_s}{4\pi} \frac{\Psi_{\text{GRB}}(z)}{1+z} \int_{L_{max}(z)}^{\infty} dL' \phi(L'), (5)$$

where $L_{max}(z) = \max\{L, L_{0.4}(z)\}$ and $L_{0.4}(z)$ is the minimum luminosity of a burst exploding at redshift z able to trigger *Swift*, i.e. $P(L_{0.4}, z) = 0.4$ ph s^{-1} cm^{-2} in the 15-150 keV BAT band[†].

We compare model predictions with the number of

[†] We have assumed here a trigger threshold of 0.4 ph s^{-1} cm^{-2} for which the *Swift*/BAT sample is complete: indeed, we find that the observed differential peak flux distribution of *Swift* GRBs

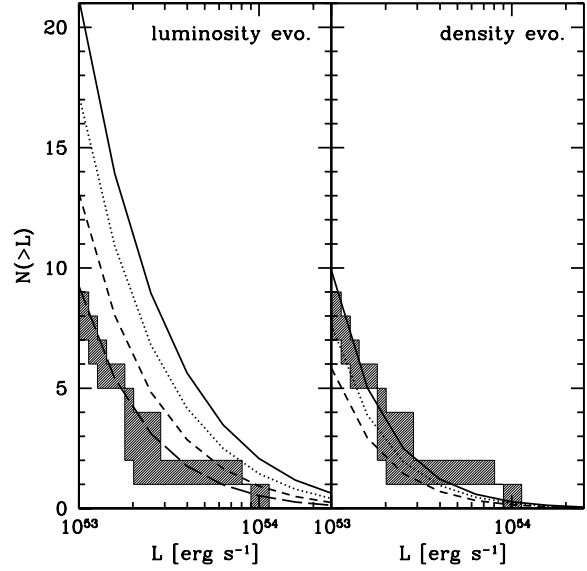


Figure 2. The cumulative number of luminous GRBs detected by *Swift* in three years of operations is shown with the histogram as a function of the isotropic equivalent peak luminosity, L . Shaded area takes into account the errors on the determination of L . Note that the data are to be considered as lower limits of the real number of *Swift* detections, since only bursts with measured redshift and peak energy are included in our sample. Pure luminosity (density) evolution models are shown in the left (right) panel. Lines as in Fig. 1. A field of view of 1.4 sr for *Swift*/BAT is adopted.

bright bursts detected by *Swift* in three years of mission. Conservatively, our data sample contains only bursts with a good redshift measurement and whose peak energy was measured or well constrained by *Swift* itself or other satellites (such as HETE-2 or Konus-Wind). We find nine GRBs[‡] detected by *Swift* with $L \geq 10^{53}$ erg s^{-1} in three years of mission. We want to stress here that this number represents a conservative lower limit on the real number of bright GRBs detected, since some luminous bursts without z and/or E_p can be present in the *Swift* catalogue. In particular, we note that a good redshift determination is obtained for $\sim 1/3$ of *Swift* bursts and for only a fraction of these we have a well constrained E_p . The cumulative distribution of the known bright bursts is shown in Fig. 2. The shaded area takes into account errors on the determination of L . The model results for the pure luminosity (density) evolution models are plot-

below this threshold is less populated than what expected from fitting the BATSE data (see also SC07).

[‡] Six out of the nine GRBs included in our sample are reported in Rossi et al. (2008): GRB 050401, GRB 050603, GRB 060927, GRB 061007, GRB 061121, and GRB 071020. In this work we use the peak luminosity computed on a 1 s timescale. We add to these other three bursts that are not present in Rossi et al. (2008) compilation: GRB 050505 with $L = 1.6 \pm 1.0 \times 10^{53}$ erg s^{-1} , GRB 060210 with $L = 4.6 \pm 2.8 \times 10^{53}$ erg s^{-1} , and GRB 060124 with $L = 1.1 \pm 0.1 \times 10^{53}$ erg s^{-1} (Romano et al. 2006). We note that the peak fluxes of all of the nine bursts considered in our sample are well above the assumed trigger threshold of *Swift*/BAT.

ted in the left (right) panel of Fig. 2. We have also checked that our findings do not depend on the assumed $L - E_p$ correlation: considering a mean break energy (as done in SC07) for all bursts does not change significantly our results.

For the pure luminosity evolution scenario, all models here considered predict a large number of bright bursts to be detected by *Swift*. Indeed, they can easily account for the observed number of bursts with $L > 10^{53}$ erg s $^{-1}$. On the other hand, models in which GRB formation is confined in low-metallicity environments seems to fall short to account for the observed bright GRBs for $Z_{th} > 0.1$. In particular, for $Z_{th} = 0.3 Z_{\odot}$, as required by collapsar models (MacFadyen & Woosley 1999; Izzard, Ramirez-Ruiz & Tout 2004), only ~ 6 bursts with $L \geq 10^{53}$ erg s $^{-1}$ should have been detected in three years of observations.

In order to test the statistical significance of our findings, we explore the parameter space around the best fit parameters looking for triple (k_{GRB} , ξ , L_0) compatible with the sure bright burst identifications. Among these, we choose the triple that give the best agreement with the differential peak flux distribution of BATSE GRBs. Then, the null hypothesis test gives us the confidence level at which we can discard the considered model. For $Z_{th} = 0.3 Z_{\odot}$, we find that null hypothesis is satisfied being, in the best case, the chance probability of ~ 0.22 . However, since we are dealing with strong lower limit on the real number of bright burst detections, we have also to consider the case in which some luminous bursts are hidden among the GRBs missing redshift and/or E_p measurement. We find that the null hypothesis probability decreases rapidly with the number of bright burst detections and already for 10 bright bursts it drops down to the percent level (see Fig. 3). So, although the $Z_{th} = 0.3 Z_{\odot}$ scenario cannot formally be discarded by available data, some degree of luminosity evolution in the GRB LF is suggested if just a few more bright bursts had to be added to our measured sample. For $Z_{th} = 0.1$ (0.2) Z_{\odot} , the models can account up to 16 (12) bright bursts in the whole *Swift* data sample, i.e. just 7 (3) ‘hidden’ bright bursts (Fig. 3). For the pure evolution scenario, we find that even a relatively large population of bright bursts hidden in the *Swift* catalogue of bursts without good redshift and/or E_p measurement, can still be accounted for.

To complete our analysis, we then consider models in which both luminosity and density evolution are present. For any value of the threshold metallicity Z_{th} , we derive the minimum luminosity evolution required to match the number of known GRBs with $L \geq 10^{53}$ erg s $^{-1}$ in the 3-year catalogue (top panel of Fig. 4). The error bars correspond to a null hypothesis probability of 1% that the model reproduces the differential peak flux distribution of BATSE GRBs. We find that for $Z_{th} > 0.3 Z_{\odot}$, the available constraints require luminosity evolution in the GRB LF. Below this threshold, models characterised by a constant LF can account for the number of known luminous bursts considering the error bars. As already pointed out, the existence of a few bright bursts hidden among GBRs without a sure redshift and/or E_p measure (more than 2/3 of the whole *Swift* catalogue), would imply the need of luminosity evolution even for lower value of Z_{th} . Moreover, note here that the existence of a distinct population of long low-luminosity GRBs at low- z (see e.g. Guetta & Della Valle 2007) strengthens our conclusions. In the form of the adopted LF (see eq. (4)), we

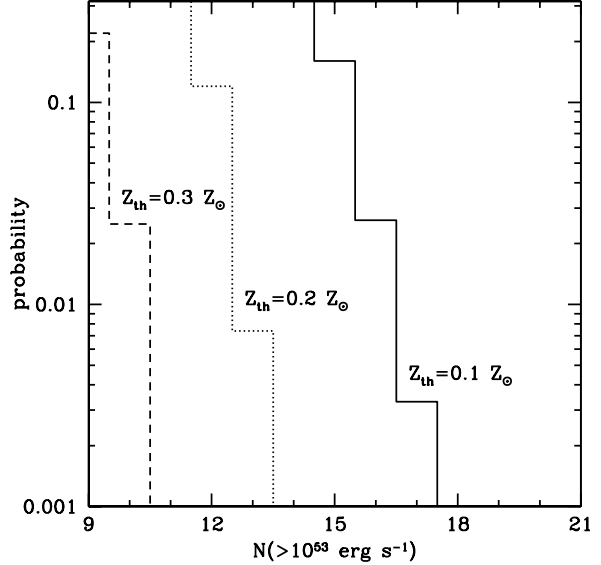


Figure 3. Chance probability to reproduce the differential peak flux distribution of BATSE GRBs given a model that predicts N bursts with $L \geq 10^{53}$ erg s $^{-1}$ in 3 years of *Swift* operations. Different pure density evolution models are plotted with different lines: dashed line for $Z_{th} = 0.3 Z_{\odot}$, dotted line for $Z_{th} = 0.2 Z_{\odot}$, and solid line for $Z_{th} = 0.1 Z_{\odot}$. The probability rapidly decreases with the number of bright bursts so that, even a few more bright bursts to be added to our conservative sample would require some degree of luminosity evolution.

do not include this population in our calculations. Should this population be statistically significant and present at all redshifts, the faint end of the LF would be more populated and all model predictions would be shifted towards lower values, increasing the discrepancy between model results and data. Since for pure density evolution models the LF cut-off luminosity is considerably larger than for pure luminosity evolution models, the former models would be more severely affected by the existence of a large population of underluminous bursts at any redshift. In conclusion, although we cannot rule out at a high confidence level pure density evolution models with $Z_{th} < 0.3 Z_{\odot}$, available data suggest some luminosity evolution in the GRB LF with redshift.

Finally, we constrain the steepness of the bright-end of the GRB LF (bottom panel of Fig. 4). Very steep LF are robustly ruled out in every model considered. We find that the maximum value of the index ξ have is $\lesssim 2.6$. For the pure luminosity evolution models, we find $\xi < 2.2$. As we already pointed out, these limits could be further constrained to explain current *Swift* data due to the possible existence of bright bursts missed by our conservative selection and of a relatively large population of faint bursts not considered here.

4 CONCLUSION

We have computed the luminosity function and the formation rate of long GRBs by fitting the observed differential peak flux distribution obtained by the BATSE satellite in two different scenarios: i) the GRB luminosity evolves with

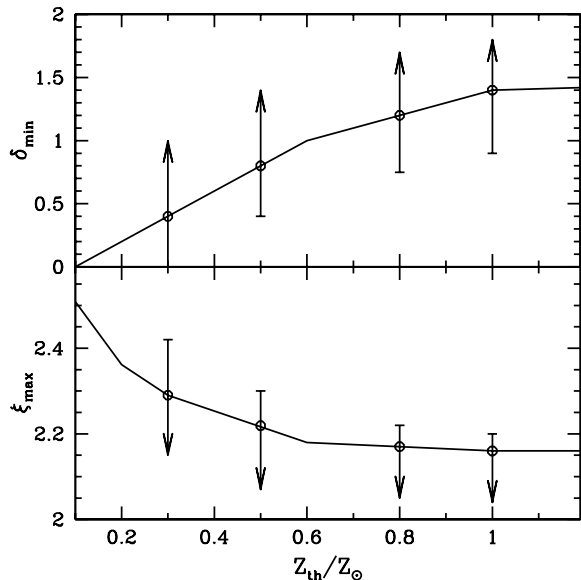


Figure 4. *Top panel:* lower limit on the luminosity evolution parameter, δ , for different threshold metallicity Z_{th} . Error bars correspond to a null hypothesis probability, that the model reproduces the differential peak flux distribution of BATSE GRBs, equal to 1%. *Bottom panel:* corresponding upper limit on the bright-end power index of the GRB LF, ξ .

redshift and ii) GRBs form preferentially in low-metallicity environments. In both cases, model predictions are consistent with the *Swift* number counts and with the number of detections at $z > 2.5$ and $z > 3.5$. To discriminate between the two evolutionary scenarios, we compared the model results against the number of luminous bursts, i.e. with peak luminosity in excess of 10^{53} erg s $^{-1}$, detected by *Swift*. Conservatively, our data sample contains only bursts with good redshift determination and measured peak energy. We find that models in which GRBs are characterised by a constant LF (i.e. for pure density evolution models) are disfavoured as they underpredict the number of luminous GRBs. *Swift* data can be explained assuming that the GRB luminosity evolves with redshift. Although we cannot discard pure density evolution models with $Z_{th} < 0.3 Z_{\odot}$ on the basis of the current sample, the existence of a few bright GRBs missed by our conservative selection criteria and/or of a relatively large population of faint GRBs would require some luminosity evolution in the GRB LF even for such low values of Z_{th} . On the other hand, pure luminosity evolution scenarios can account more easily for a large number of burst detections with $L > 10^{53}$ erg s $^{-1}$. In this work, we derive lower limits to the luminosity evolution of the GRB LF with redshift for different values of the metallicity threshold for the GRB formation. Moreover, we use these constraints to set a robust upper limit on the bright-end of GRB LF. We find that the number of bright GRBs detected by *Swift* implies that this cannot be very steep: $\xi \lesssim 2.2$ (pure luminosity evolution) and $\xi \lesssim 2.6$ (for $Z_{th} < 0.3 Z_{\odot}$).

In conclusion, we find that available *Swift* observations point towards a scenario where GRBs were more luminous in the past. Although current data sample of bright GRBs with good redshift and E_p determination is still very poor, our findings show that these data can be used to set important

constraints on the cosmic evolution of GRBs and on the steepness of their LF.

Finally, the new constraints on the GRB LF allow us to derive robust lower limits on the number of bursts detectable by *Swift* at very high redshift. Assuming a trigger threshold $P_{lim} = 0.4$ ph s $^{-1}$ cm $^{-2}$, at least $\sim 5 - 10\%$ of all detected GRBs should lie at $z \geq 5$, where the lower (upper) value refers to a pure luminosity evolution (pure density evolution with $Z_{th} = 0.1 Z_{\odot}$) model. Among these, $> 1 - 3$ GRB yr $^{-1}$ should be detected at $z \geq 6$. These lower bounds double by lowering the *Swift* trigger threshold by a factor of two (Salvaterra et al. 2008). These results are consistent with the lower limits on the number of high- z detections obtained by Salvaterra et al. (2007, 2008) using redshift distribution constraints.

REFERENCES

- Amati L. et al., 2002, A&A, 390, 81
 Amati L., 2006, MNRAS, 372, 233
 Band D.L. et al., 1993, ApJ, 413, 281
 Cen R. & Fang T., 2007, submitted to ApJL, arXiv:0710.4370
 Daigne, F., Rossi, E. M., & Mochkovitch, R. 2006, MNRAS, 372, 1034
 Gehrels, N., et al. 2004, ApJ, 611, 1005
 Ghirlanda G., Ghisellini G., Firmani C., Celotti A., Bosnjak Z., 2005, MNRAS, 360, L45
 Greiner J., et al., 2008, ApJ submitted, arXiv:0810.2314
 Guetta D. & Della Valle M., 2007, ApJ, 657, L73
 Guetta D., Piran T. & Waxman E., 2005, ApJ, 619, 412
 Hopkins A. M. & Beacom J. F., 2006, ApJ, 651, 142
 Izzard, R. G., Ramirez-Ruiz, E., Tout, C. A., 2004, MNRAS, 348, 1215
 Kaneko Y., Preece R. D., Briggs M. S., Paciasas W. S., Meegan C. A., Band D. L., 2006, ApJS, 166, 298
 Kistler M. D., Yuksel H., Beacom J. F., Stanek K. Z., 2008, ApJ, 673, L119
 Langer L. & Norman C. A., 2006, ApJ, 638, L63
 Lapi A., Kawakatu N., Bosnjak Z., Celotti A., Bressan A., Granato G.L., Danese L., 2008, MNRAS, 386, 608
 Li L.-X., 2007, MNRAS in press, arXiv:0710.3587
 Lloyd-Ronning N.M., Fryer C. & Ramirez-Ruiz E., 2002, ApJ, 574, 554
 MacFadyen, A., & Woosley, S., 1999, ApJ, 524, 262
 Mészáros, P. 2006, Reports of Progress in Physics, 69, 2259
 Natarajan, P., Albanna, B., Hjorth, J., Ramirez-Ruiz, E., Tarvir, N., & Wijers, R. 2005, MNRAS, 364, L8
 Preece R. D., Briggs M. S., Malozzi R. S., Pendleton G. N., Paciasas W. S., & Band D. L., 2000, ApJS, 126, 19
 Romano P. et al., 2006, A&A, 456, 917
 Rossi F. et al., 2008, MNRAS in press, arXiv:0802.0471
 Salvaterra R. & Chincarini G., 2007, ApJ, 656, L49 (SC07)
 Salvaterra R., Campana S., Chincarini G., Tagliaferri G., Covino S., 2007, MNRAS, 380, L45
 Salvaterra R., Campana S., Chincarini G., Covino S., Tagliaferri G., 2008, MNRAS, 385, 189
 Stark D. P., Bunker A. J., Ellis R. S., Eyles L. P., Lacy M., 2007, ApJ, 659, 84
 Stern B. E., Tikhomirova Y., Stepanov M., Kompaneets D., Berezhnoy A., Svensson R., 2000, ApJ, 540, L21
 Yonetoku D., Murakami T., Nakamura T., Yamazaki R., Inoue A. K., Ioka K., 2004, ApJ, 609, 935
 Wei D. M. & Gao W. H., 2003, MNRAS, 345, 743